symmetry

MDPI

Article

Analysis on the Effect of Phase Noise on the Performance of Satellite Communication and Measurement System

Xuan Liu [1,2], Hongmin Lu [1], Yifeng He [2], Fulin Wu [1], Chengxi Zhang [3] and Xiaoliang Wang [4,*]

[1] School of Electronic Engineering, Xidian University, Xi'an 710071, China
[2] China Academy of Space Technology, Xi'an 710100, China
[3] School of Internet of Things Engineering, Jiangnan University, Wuxi 214082, China; cxzhang@jiangnan.edu.cn
[4] School of Aeronautics and Astronautics, Shanghai Jiao Tong University, Shanghai 200240, China
* Correspondence: xlwang12321@sjtu.edu.cn

Abstract: An oscillator is a key component of a satellite communication measurement and control system, performing symmetry precisely as a time frequency reference. At the same time, the phase noise index has a close coupling relationship with the overall performance of the entire system, while persistently breaking the symmetry property of the oscillator during work. It is very important to study and reasonably allocate the phase noise index. According to the theoretical formula of phase noise, this paper analyzes the power law spectral model in the frequency domain and the noise jitter characteristics in the time domain. Using the carrier tracking loop in the measurement system, the frequency domain transfer model of phase noise is established, and typical analysis results are given. A discrete fractional integration algorithm is proposed, which can generate the phase noise time domain sequence under the given power law spectral model coefficients. The proposed algorithm is more realistic compared with the previous numerical calculation method, and has sufficient accuracy compared with the results of the instrument. After frequency domain conversion, the RMS deviation between the simulated noise sequence in the frequency domain and the measured single sideband power spectral density is less than 2.5 dB, indicating that the phase noise sequence can reflect the frequency domain characteristics more completely. A communication measurement simulation system is built, and a discrete sequence simulation analysis method combining frequency domain and time domain is provided, and the coupling relationship of key indicators such as phase noise, thermal noise, communication data rate, modulation method and bit error rate is synthesized. The results show that the BER of the QPSK/BPSK communication system will not be significantly reduced if the phase jitter RMS caused by the phase noise is less than 5 degrees, so 5 degrees can be used as a reference for the decomposition of the carrier SSB phase noise index. The simulation results have been successfully applied to a satellite inter-satellite link system, which has universal practical application value.

Keywords: phase noise; noise jitter characteristics; oscillator; QPSK; BPSK

check for updates

Citation: Liu, X.; Lu, H.; He, Y.; Wu, F.; Zhang, C.; Wang, X. Analysis on the Effect of Phase Noise on the Performance of Satellite Communication and Measurement System. *Symmetry* **2023**, *15*, 2053. https://doi.org/10.3390/sym15112053

Academic Editor: Christos Volos

Received: 7 October 2023
Revised: 1 November 2023
Accepted: 7 November 2023
Published: 12 November 2023

Copyright: © 2023 by the authors. Licensee MDPI, Basel, Switzerland. This article is an open access article distributed under the terms and conditions of the Creative Commons Attribution (CC BY) license (https://creativecommons.org/licenses/by/4.0/).

1. Introduction

Oscillators (or atomic clocks) are widely used in radar, communications, navigation, robot control and metrology electronic systems. Affected by the oscillator circuit itself and the external environment, their frequency or phase is constantly changing with the disappearing symmetry property, which affects the function and performance of the communication or measurement system. The phase noise of an oscillator is a key measure of oscillator performance. In the frequency domain, phase noise appears as a sideband spectrum distributed on both sides of the carrier signal, and in the time domain, it appears as phase jitter. Taking the communication system as an example, the phase noise of the received signal and the phase noise of the local oscillator signal are transmitted during the up-conversion process, so that the transmitted signal and the baseband signal to be

processed contain a large amount of phase noise, which affects the anti-interference ability of the transceiver system and the reception. The signal-to-noise ratio of the signal will eventually result in bit errors. Therefore, it is very important to study and reasonably allocate phase noise indicators.

In the field of satellite radio technology, there are more and more payload systems that couple communication and measurement functions, such as satellite navigation systems, formation satellite inter-satellite link systems and deep space exploration satellite-ground link systems. Previous studies on the performance of communication measurement systems focused on the analysis of thermal noise, focusing on the coupling relationship between the carrier-to-noise ratio and bit error rate. In recent years, scholars have gradually begun to study the influence of phase noise on the comprehensive performance of communication measurement. The authors of [1] analyzed the influence of phase noise on the performance of relay satellite TDRSS data transmission systems, and initially gave the relationship between phase noise and bit error rate. The authors of [2] analyzed the influence of the phase noise of the receiver's local oscillator on the communication performance and gave a BER prediction algorithm in the case of abrupt changes in the phase noise. The authors of [3,4] focused on the effect of phase noise on the demodulation performance of the receiver under QPSK modulation. The authors of [5] present a method to suppress common-mode phase error and inter-carrier interference caused by phase noise in full-duplex OFDM systems. The simulation results show that compared with the traditional SI elimination scheme, the proposed method has significantly improved the SI elimination capability. Based on theoretical analysis and experimental research, the authors of [6] compared the influence of two local oscillator signals with different phase noise characteristics on the reception bit error rate (BER) performance of communication systems and found that the near phase noise of the local oscillator signal source has a significant effect on the bit error rate performance. In addition, the method of selecting the digital phase-locked loop bandwidth at the receiving end to suppress the phase noise of the local oscillator signal source is discussed. The authors of [7] discussed the phase noise problem in millimeter wave systems, and reviewed various emerging phase noise problems and corresponding solutions for future 5G wireless networks. A new pilot-assisted estimation and compensation (PEC) method is proposed to reduce phase noise, and the suppression ability of this method on phase noise in millimeter wave and microwave systems is comprehensively compared. The authors of [8] proposed a communication transceiver design method which can effectively reduce the phase noise contained in the multi-run interference components. Simulation results show that the proposed transceiver design can extend the transmit power, relax the requirement of the analog eliminator, and show advantages in the application scenarios of a high transmit power long-distance communication or analog eliminator.

Other works of literature about phase noise include the work of [9], in which CMOS voltage-controlled oscillators (VCO) with a frequency range of 22.7 GHz–27.9 GHz are described. At 1 MHz offset frequency, the power consumption is 1.35 mW and the phase noise is as low as 117 dBc/Hz regular results, which provides a reference for the application design of low-power and low-phase-noise aerospace devices. The authors of [10] focus on the damage of phase noise to the performance of an orthogonal frequency partition multiplexing (OFDM) system. A low complexity blind data detector based on the maximum a posteriori (MAP) criterion is proposed. In [11], a phase noise frequency synthesis method based on phase-locked loop is proposed, which can effectively improve the level of phase noise and improve the performance of the communication system. This method has the potential to be realized by FPGA, and can be applied to the signal processor of digital communication system. The authors of [12] address the issue of polar coding design for bit-interleaved coded modulation (BICM) systems over the phase noise channel. The polarization code is constructed from the calculated average GMI per bit layer for a given PRE-variance and signal-to-noise ratio (SNR). The superior performance of the phase noise matching polarity design is verified by comparing it with the channel mismatch design (8PSK). The data show that this algorithm can be applied to QPSK, 16APSK and

higher order communication systems. Moreover, the authors of [13] explore the impact of EEPN scale increases with the increase in the fiber dispersion, laser linewidths, symbol rates, signal bandwidths and the order of modulation formats. A 28-Gsym/s QPSK optical transmission system with a significant EEPN has been implemented. The measured results show that the RF pilot tone can entirely eliminate the LPN and efficiently suppress the EEPN when it is applied prior to the CPR. The authors of [14] provide a reference for the multi-rate and multi-modulation comparison simulation in this paper. The influence of carrier phase noise on the performance of modulation and demodulation in satellite communication downlink is simulated and analyzed. The conclusion is that the influence of carrier phase noise on performance of the specified modulation mode is related to the sampling rate and symbol rate of the receiver. In [15], a testbed based on USRP and 60 GHz Tx/Rx RF front-ends is developed to research a phase noise cancellation (PNC) scheme, which achieves −20 dB EVM data transmission for real-time video streaming. The authors of [16] indicate a corresponding noise gauging function (NGF) which can make relatively sharp differentiation between error-causing and non-error-causing noise vectors. This function can be used to judge the accuracy of EVM measured by the instrument.

In these related papers, phase noise is suppressed and canceled through various methods, while the phase noise itself is not fully modeled and quantified. In addition, in most of these studies, the magnitude of the phase noise is set, and the phase fluctuation is evaluated by the root mean square. For example, the standard deviation of the phase noise is 5°, and then a conclusion is drawn based on the transmission model using numerical analysis or theoretical calculation methods. This paper is based on an inter-satellite link system in orbit, which combines high precision carrier measurement and high rate communication, and is a satellite payload with high comprehensive performance. The main purpose of this thesis is to quantitatively analyze the phase jitter of the reference frequency signal and RF microwave signal by means of the time domain and frequency domain. In the frequency domain, the phase jitter is analyzed by the numerical method. In the time domain, a noise power spectrum conversion algorithm based on IIR is proposed, which converts the noise power spectrum into the time domain noise sequence. The effect of phase noise on the performance of the digital communication system is simulated and analyzed in the time domain sequence. Several commonly used parameter indexes are given, which can be used as a reference for system parameter design.

2. Theory Introduction

2.1. Phase Noise

In general, the mathematical model of the oscillator output signal can be expressed as the following:

$$V_o(t) = A\sin(2\pi f_o t + \phi(t)) \quad (1)$$

The amplitude noise caused by the amplitude fluctuation is omitted. $\phi(t)$ in the phase term represents all phase and frequency deviations from the nominal frequency f_o and phase $2\pi f_o t$, which can be called phase perturbations. There are two reasons for introducing $\phi(t)$: one is the initial offset of the oscillator frequency and the drift of the frequency with time caused by causal elements such as ambient temperature changes and device aging, which mainly affect the medium and long-term frequency stability of the oscillator output signal. The other is the random phase fluctuation caused by random factors such as thermal noise and flicker noise inside the device, which mainly affect the short-term frequency stability of the oscillator. Phase noise is the random fluctuation of the oscillator phase caused by this random factor. This random fluctuation causes the signal spectrum to no longer be an infinite impulse function, as sidebands appear at the center frequency, causing spectrum spread, as shown in Figure 1 below.

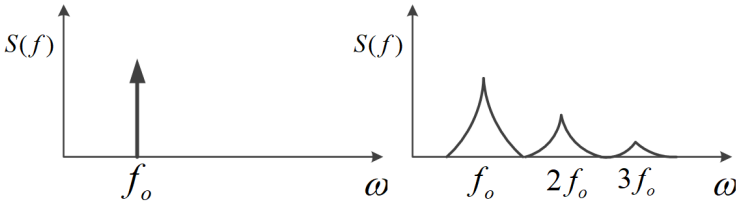

Figure 1. Spectral spreading due to phase noise. (The left is the ideal spectrum, the right is the actual output spectrum).

To characterize phase noise, the following two basic concepts are introduced: instantaneous relative frequency offset $y(t)$ and instantaneous relative phase offset: $x(t)$

$$y(t) = \frac{1}{2\pi f_o}\frac{\mathrm{d}\phi(t)}{\mathrm{d}t} \tag{2}$$

$$x(t) = \frac{\phi(t)}{2\pi f_o} \tag{3}$$

Characterization of phase noise can be performed in the time and frequency domains, respectively. The commonly used characterization method in the time domain of phase noise is in the form of the Allan variance [17]:

$$\sigma^2(\tau) = \frac{1}{2} < (y_{k+1} - y_k)^2 >= \frac{1}{2\tau^2} < (x_{k+2} - 2x_{k+1} + x_k)^2 > \tag{4}$$

τ is the sampling interval of the Allan variance (such as 1 s, 10 s . . . 1000 s, etc.). y_k and x_k represent the discrete sequences obtained by sampling the instantaneous relative frequency offset and phase offset at intervals of τ, respectively. The method of characterizing phase noise in the frequency domain is mainly the method of power spectral density. The power spectral density of phase noise is generally expressed as $S_\phi(f)$. Phase noise has a strictly one-way mathematical relationship to the Allan variance. Among the methods for quantifying phase noise, the single-sideband power spectral density $L(f)$ is the most commonly used indicator for the characterization of phase noise in the frequency domain, and it is also the result given by a general phase noise analyzer. $L(f)$ is defined as the ratio of the single-sideband noise power to the carrier signal power of the oscillator output signal within a 1 Hz bandwidth off-center carrier frequency $\Delta f(Hz)$, as in Figure 2. When in decibel form, the unit of $L(f)$ is dBc/Hz. When the amplitude of $\phi(t)$ is much less than 1 rad, $L(f)$ and $S_\phi(f)$ have the following relationship, in which the unit does not include dB.

$$L(\Delta f) = 10\log_{10}\left[\frac{P_{SSB}(f_0 + \Delta f, 1Hz)}{P_S}\right] \tag{5}$$

$$L(f) = 10\log_{10}\left(\frac{1}{2}(S_\phi(f))\right) \tag{6}$$

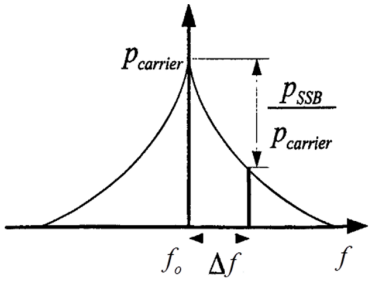

Figure 2. Definition of phase noise.

2.2. Frequency Domain Representation

The most mature model for the quantitative description of oscillator phase noise is the power law spectrum model established according to the experimental results and the internal characteristics of the oscillator as Figure 3, that is, the oscillator phase noise spectral density can be expressed as [18]

$$S_\phi(f) = \sum_{i=0}^{4} \frac{h_i}{f^i} = h_0 + \frac{h_1}{f} + \frac{h_2}{f^2} + \frac{h_3}{f^3} + \frac{h_4}{f^4} \tag{7}$$

Among them, the corresponding noise components are as follows: h_0 is called white phase modulation noise (WPM), h_1 is called flicker phase modulation noise (FPM), h_2 is called white frequency modulation noise (WFM), h_3 is called flicker frequency modulation noise (FFM) and h_4 is called frequency modulation random walk noise (RWFM). Among the five noise components, except WPM, the other four are non-stationary processes. An important property of 1/f noise is self-similarity or scale invariance. The meaning of Equation (7) in the time domain means that the phase noise inside the oscillator can be expressed as the superposition of five mutually independent power law spectral noise components.

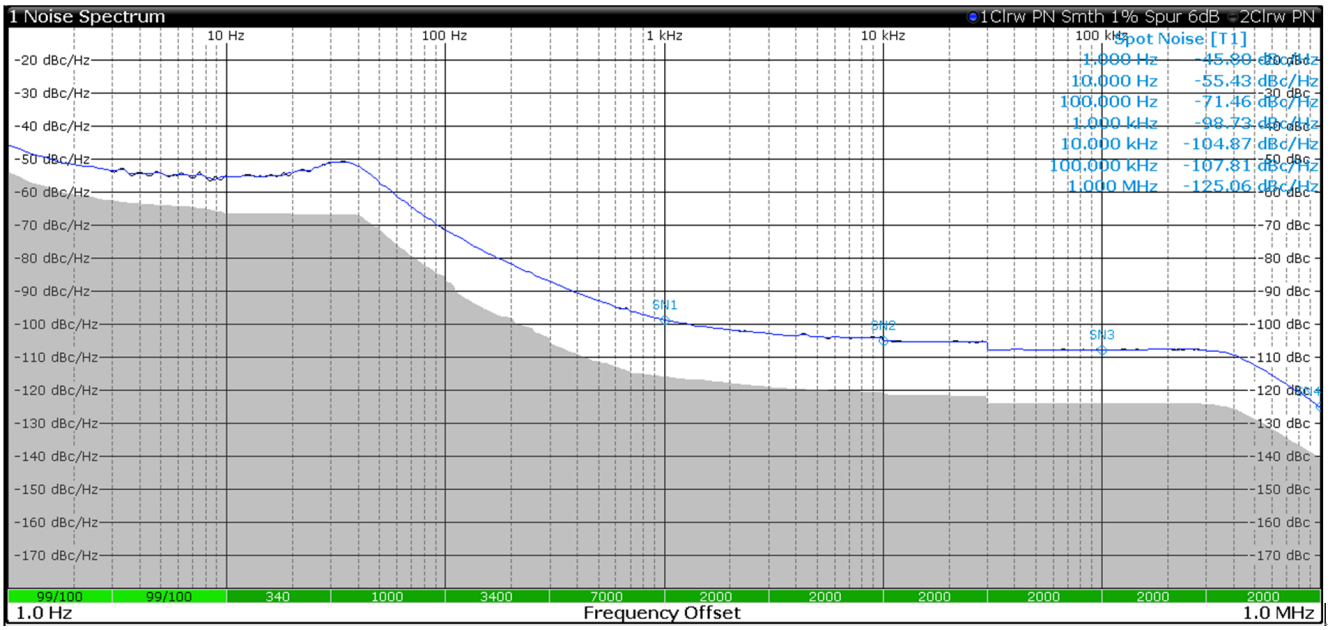

Figure 3. Typical Ka signal phase noise test results. (Rohde Schwarz FSW50 Phase Noise Analyzer).

The research and application of the power law spectral model in this paper is reflected in two points:

(1) According to a set of measured SSB phase noise points, through the fitting algorithm, the power law coefficient can be solved, and Formula (7) can be established. In this way, the phase noise characteristics of this signal can be clearly described from the frequency domain. If the transfer function of a signal in a communication measurement system is known, various errors caused by phase noise after the signal containing phase noise is transmitted can be solved. This analysis method is carried out in the frequency domain and is described in Section 3.

(2) Assuming that Equation (7) has been established and the frequency domain characteristics of the phase noise of the signal are known, an algorithm can be designed to generate the time domain of the phase noise corresponding to the corresponding power law spectral components based on the weight coefficients of each power law spectral component noise. The time-domain phase noise sequence can be obtained by superimposing each component in the time domain. This is very critical and useful.

In any time series communication measurement system simulation model, the time domain noise sequence can be superimposed on the pure carrier to simulate the signal with phase noise generated by the actual link. This method of analysis is performed in the time domain and is highlighted in Section 4.

2.3. Time Domain Representation

The mathematical model of phase jitter (expression in time domain) caused by various phase noises in Figure 4 is shown in Equation (8). This formula can be used to simply calculate the phase jitter of the signal corresponding to a given phase noise sequence. The resulting phase jitter sum is actually approximately equal to the RMS value of the phase jitter noise sequence exhibited in the time domain of this signal

$$J = \frac{\sqrt{2 \cdot \int_{f_L}^{f_H} L_\phi(f) \cdot \mathrm{d}f}}{2 \cdot \pi} \tag{8}$$

$$J_{UI} = \sqrt{J_{WPM}^2 + J_{FPM}^2 + J_{WFM}^2 + J_{FFM}^2 + J_{RWFM}^2} \tag{9}$$

Among Formula (9), $L(f)$ is the SSB phase noise curve (dBc/Hz); J is the phase jitter in the frequency range $f_L \sim f_H$, unit: cycle; and J_{UI} is the sum of the phase jitter in the spectral range of interest, unit: cycle.

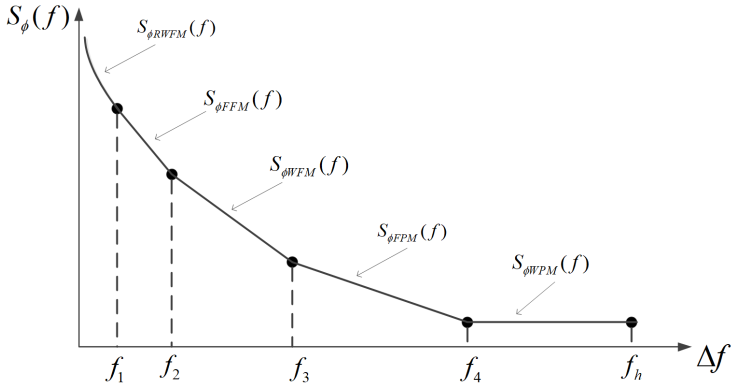

Figure 4. Phase noise power spectral density. (Power law spectrum model).

Table 1 provided a set of phase noise data from test, and Figure 5 interpreted in visual. Moreover, Table 2 demonstrated the phase noise results by using segment method.

Table 1. A set of typical phase noise measurements.

Frequency Offset	Phase Noise
1 Hz	≤ -34 dBc/Hz
10 Hz	≤ -51 dBc/Hz
100 Hz	≤ -63 dBc/Hz
1 KHz	≤ -75 dBc/Hz
10 KHz	≤ -95 dBc/Hz
100 KHz	≤ -101 dBc/Hz
1 MHz	≤ -120 dBc/Hz

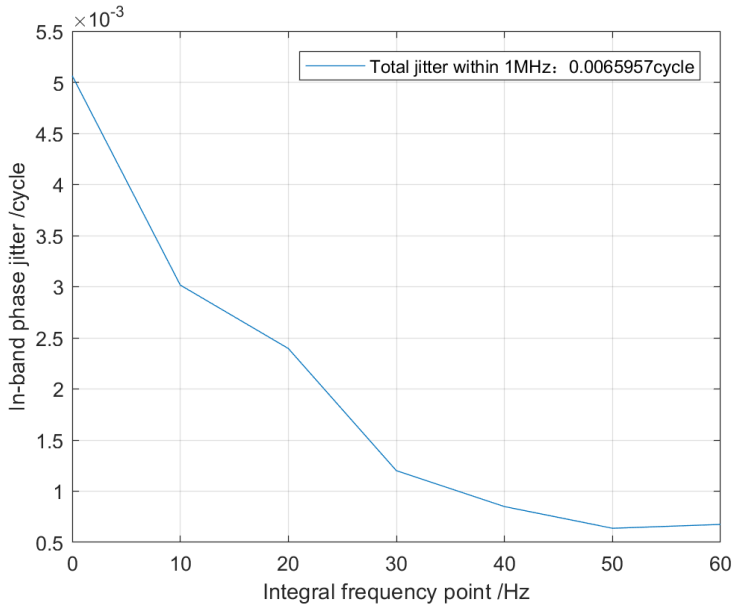

Figure 5. Phase jitter calculated according to Table 1. (The frequency deviation within 10 KHz occupies more than 80% of the total error).

Table 2. Phase noise parameters in each frequency offset range (segment method).

Frequency (Hz)	$L(f)$ (dBc/Hz)	$S_\phi(f)$ (rad^2/Hz)
1∼10	$(-34-51)/2$	5.62×10^{-5}
10∼100	$(-51-63)/2$	2.00×10^{-6}
100∼1 K	$(-63-75)/2$	1.26×10^{-7}
1 K∼10 K	$(-75-95)/2$	3.16×10^{-9}
10 K∼100 K	$(-95-101)/2$	1.58×10^{-10}
100 K∼1 M	$(-101-120)/2$	8.91×10^{-12}
1 M∼10 M	-120	1.00×10^{-12}

3. Impact Analysis of Phase Noise in Frequency Domain

Taking a two-satellite formation satellite inter-satellite ranging system as an example, the application of a phase-noise power law spectral model in frequency domain analysis is analyzed. The core of the ranging system to generate the measurement value is the pseudo code and carrier tracking loop, and the loop tracking error corresponds to the accuracy of the measurement value. Here, we take the phase-locked loop of carrier tracking as an example.

Let $H(f)$ be the system transfer function of the phase-locked loop, as shown in Figure 6, $E(f) = 1 - H(f)$ be the error transfer function, $S_{psi}(f)$ be the phase noise power spectral density of the input signal, and $S_{poi}(f)$ be the phase noise power spectral density of the local oscillator, then the total error spectrum can be expressed as [19]:

$$S_{po}(f) = (S_{psi}(f) + S_{poi}(f))|E(f)|^2 = S_{pi}(f)|E(f)|^2 \tag{10}$$

The error variance of phase tracking is expressed as:

$$\sigma_\theta^2 = \int_0^\infty S_{po}(f)\mathrm{d}f = \int_0^\infty S_{pi}(f)|E(f)|^2\mathrm{d}f \tag{11}$$

When the loop bandwidth is very narrow (within 5 Hz), the first two low-order noises (corresponding to high-frequency noises) in Equation (7) can be ignored, and the latter three types of phase noise dominate the final tracking accuracy. The carrier tracking loop

of the inter-satellite link system uses a third-order phase-locked loop, and its error transfer function can be expressed as:

$$|E(\omega)|^2 = |1 - H(\omega)|^2 = \frac{\omega^{2n}}{\omega^{2n} + \omega_L^{2n}}, n = 3 \tag{12}$$

Among Equation (12), ω_L represents the loop bandwidth (Hz). By substituting Equation (12) into Equation (11), the tracking error of the third-order phase-locked loop can be obtained as:

$$\sigma_\theta = \sqrt{2}\pi f_0 [\frac{\pi^2 h_4}{3\omega_L^3} + \frac{\pi h_3}{3\sqrt{3}\omega_L^2} + \frac{h_2}{6\omega_L}] 1/2 \ (rad) \tag{13}$$

According to Equation (13), when the phase noise power law spectrum parameters of the measured signal are known, the tracking error caused by the phase noise under a certain loop bandwidth parameter can be calculated.

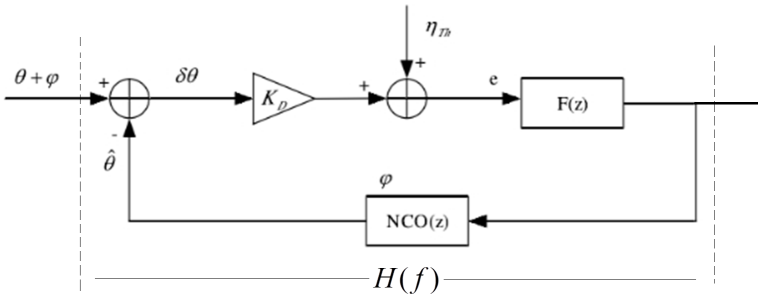

Figure 6. Composition and error transfer schematic of carrier tracking loop.

Assuming that the inter-satellite link system receives a signal with a carrier-to-noise ratio of 75 dBHz, the selected reference source is a constant temperature crystal oscillator (OCXO), and the power law spectrum parameters are shown in Table 3. Usually, the power law spectral coefficients can also be obtained by a fitting algorithm based on the measured phase noise curve or the phase noise index.

Table 3. Power law spectrum parameters of a typical oscillator or atomic clock.

Type	h_2	h_3	h_4
TCXO	1.00×10^{-21}	1.00×10^{-20}	2.00×10^{-20}
OCXO	2.51×10^{-26}	2.51×10^{-23}	2.51×10^{-22}
Rubidium clock	1.00×10^{-23}	1.00×10^{-22}	1.30×10^{-26}
Cesium clock	2.00×10^{-20}	7.00×10^{-23}	4.00×10^{-29}

The final tracking errors can be obtained as shown in Figure 7 below. It can be seen that the phase-locked loop presents a low-pass characteristic to thermal noise (described by the carrier-to-noise ratio index), and the smaller the loop bandwidth, the smaller the tracking error introduced by the thermal noise. The phase-locked loop presents a high-pass characteristic of the phase noise. The larger the loop bandwidth, the smaller the tracking error caused by the phase noise. Accordingly, it is necessary to comprehensively select the loop bandwidth according to the actual system measurement accuracy index.

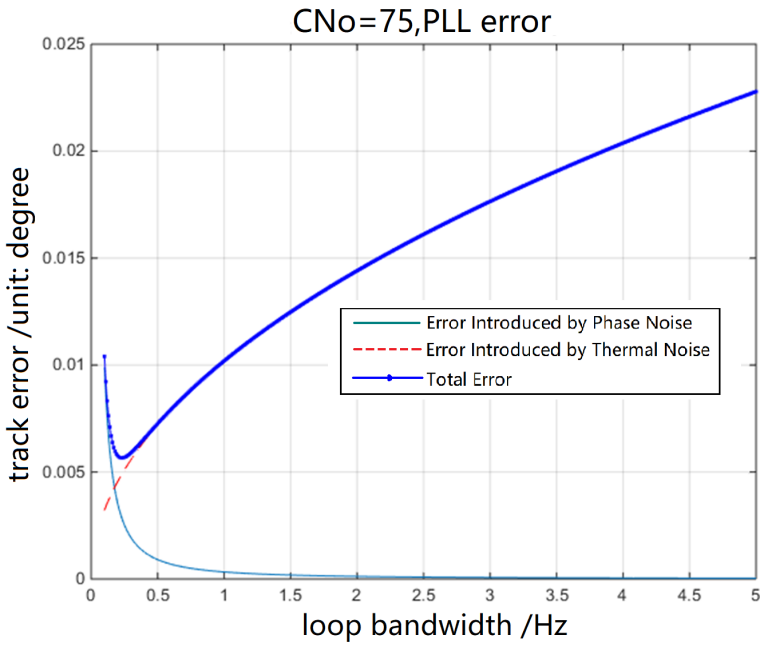

Figure 7. Tracking error introduced by thermal noise and phase noise of third-order PLL.

4. Impact Analysis of Phase Noise in Time Domain

According to the power law spectral model of phase noise, the purpose of simulating the phase noise sequence in the time domain is to generate various power law spectral component noises, the most critical of which is the generation of 1/f noise components.

Time-domain simulation methods for power law spectral noise can be divided into three categories [20]: methods based on autoregressive moving average (ARMA) models, models based on discrete fractional integration and models based on wavelet analysis. The noise generated by the method based on ARMA is stationary and has no scale invariance, and this generation method is not easy to operate in practical use. Due to the inherent time-frequency analysis characteristics of wavelets, the noise sequence generated by wavelets is non-stationary and to scale. Invariant phase noise sequences generated by discrete fractional integration methods are also ideally non-stationary and scale invariant, and are easy to manipulate in practice. Based on the above analysis, considering that the discrete fractional integration method has mature mathematical models available in the MATLAB system (essentially an extension of the IIR filter), it is proposed to use the fractional integration-based method to generate phase noise sequences.

Generating the components $1/f^{\alpha}$ using the discrete fractional integration method is based on the Brownian motion model with one-dimensional discrete random walk characteristics, and its transfer function can be approximately expressed as [21,22]

$$H(z) = \frac{1}{(1 - z^{-1})^{\alpha}} \tag{14}$$

Assuming that the sampling step size of the simulation is Δt, according to the signal processing theory, the white noise sequence with variance Q_d passes through the discrete system, and the power spectral density of the continuous noise corresponding to the output sequence can be obtained as

$$S(f) = \frac{Q_d \Delta t}{(2\sin(\pi f \Delta t))^{\alpha}} \tag{15}$$

In order to facilitate the simulation of discrete systems, (14) is expanded according to the series, and we get

$$H(z) = \frac{1}{1 - \frac{\alpha}{2}z^{-1} - \frac{\alpha(1-\alpha)}{2}z^{-2} - \dots} \tag{16}$$

This transfer function is equivalent to the IIR filter given by

$$x_n = -a_1 x_{n-1} - a_2 x_{n-2} - a_3 x_{n-3} - \dots + w_n \tag{17}$$

The filter coefficients are expressed as

$$\begin{aligned} a_0 &= 1 \\ a_k &= (k - 1 - \alpha)\frac{\alpha}{k} \end{aligned} \tag{18}$$

In order to facilitate modeling in MATLAB, the series of infinite IIR needs to be truncated. After many calculations, the frequency decade N at which the noise sequence generated by the truncated IIR filter exhibits the desired power law spectral characteristics has the following approximate relationship with the series n of the IIR filter:

$$N = \log_{10}(n) + 1 \tag{19}$$

The following simulation example is implemented for a certain type of OCXO crystal oscillator (5 MHz). The phase noise power spectral density curve of the crystal oscillator is basically white noise above 1 KHz, as shown in Figure 8 below. According to Nyquist's theorem, combined with the simulation efficiency, the sampling frequency of the phase noise time-domain sequence can be set as 100 KHz. Typical values in Figure 8 are extracted into Formula (7) and the synthetic time-domain phase noise sequence of each component corresponding to the power law spectrum model is simulated according to the fractional-order integration algorithm, as in Figure 9. Figure 10 is the time-domain sequence corresponding to each power law spectral component. Figure 11 is the phase noise single-side single-power spectrum model calculated by Figure 9, and the analysis result is highly consistent with the measured result in Figure 8.

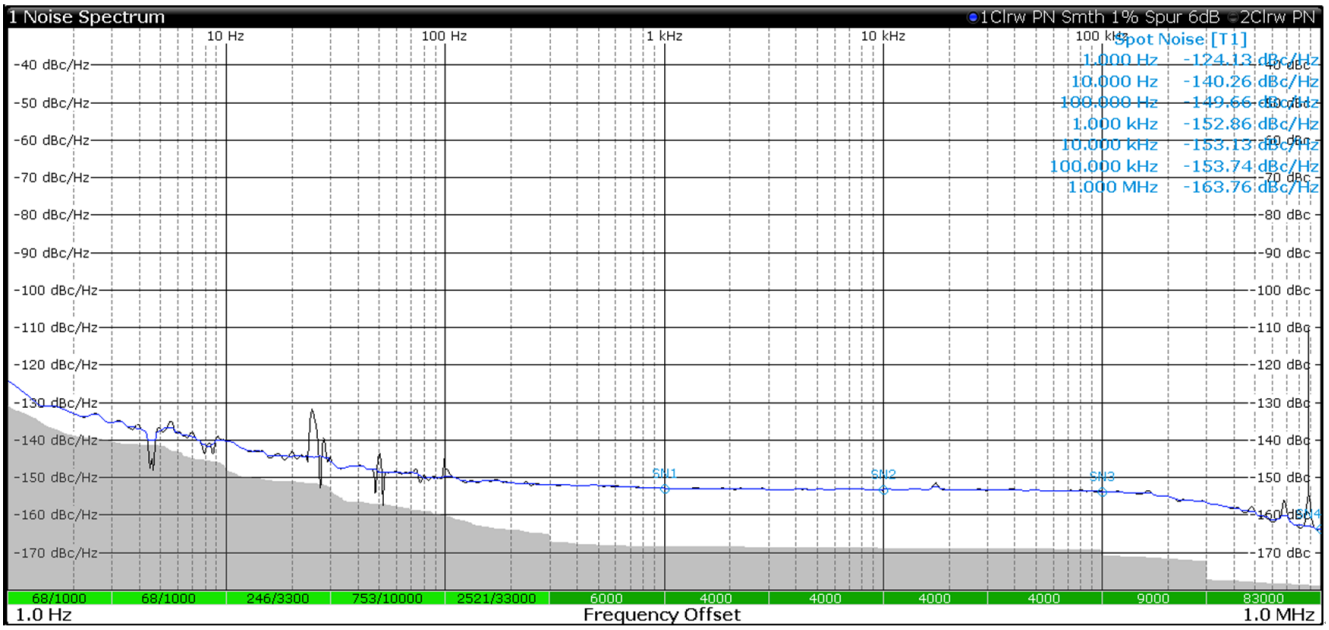

Figure 8. Phase noise measurement of 5 MHz OCXO.

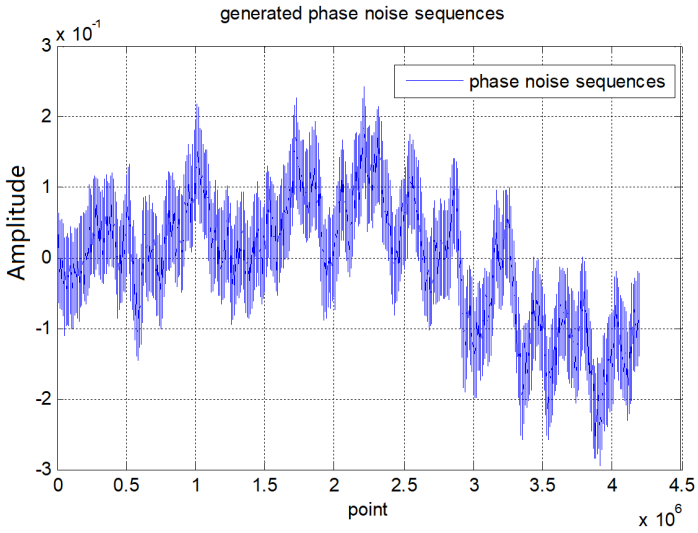

Figure 9. Phase noise time-domain sequence curve of 5 MHz OCXO.

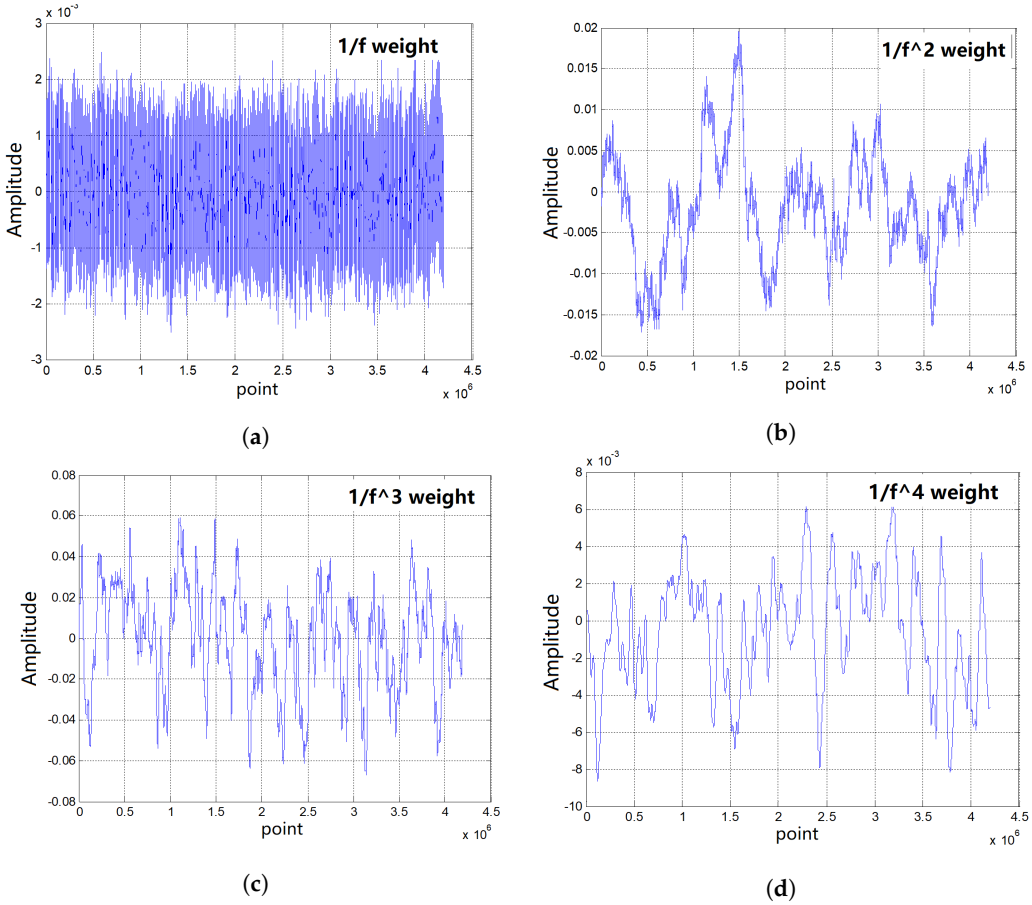

Figure 10. Phase noise time-domain sequence curve of 5 MHz OCXO. (**a**) Time domain noise corresponding to $1/f$ power law coefficients; (**b**) time domain noise corresponding to $1/f^2$ power law coefficients; (**c**) time domain noise corresponding to $1/f^3$ power law coefficients; (**d**) time domain noise corresponding to $1/f^4$ power law coefficients.

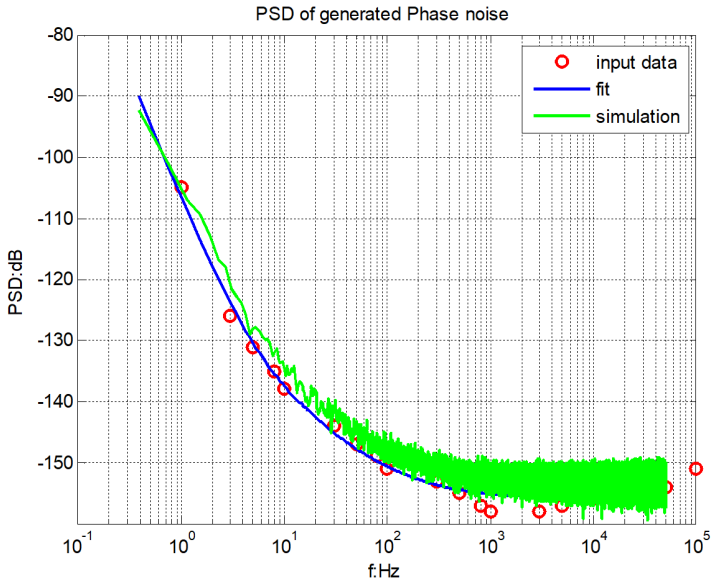

Figure 11. Phase noise power spectral density simulation curve based on Figure 9.

5. Modelling of Communication Measurement Systems

5.1. Model Design

The comprehensive simulation system for communication measurement is built based on Simulink, as shown in Figure 12 below, including transmitting, analog-to-digital conversion, matched filtering, carrier synchronization, symbol synchronization and other modules, which can realize modulation modes such as BPSK, QPSK, OQPSK and QAM [23,24]. In the transmitter model, the phase noise time-domain generation model in Section 4 is entered into the system, and the coefficients of the phase-noise power law spectrum are changed to generate the original transmit signal containing the phase-noise time-domain sequence with the corresponding amplitude (measured by the root mean square of the noise). The Carrier Synchronization Loop module includes the phase noise transfer model introduced in Section 3, and has the ability to analyze the carrier loop performance under large dynamic conditions between satellites. The sampling rate of the simulation system is variable and can be set to 50 KHz∼50 MHz as needed.

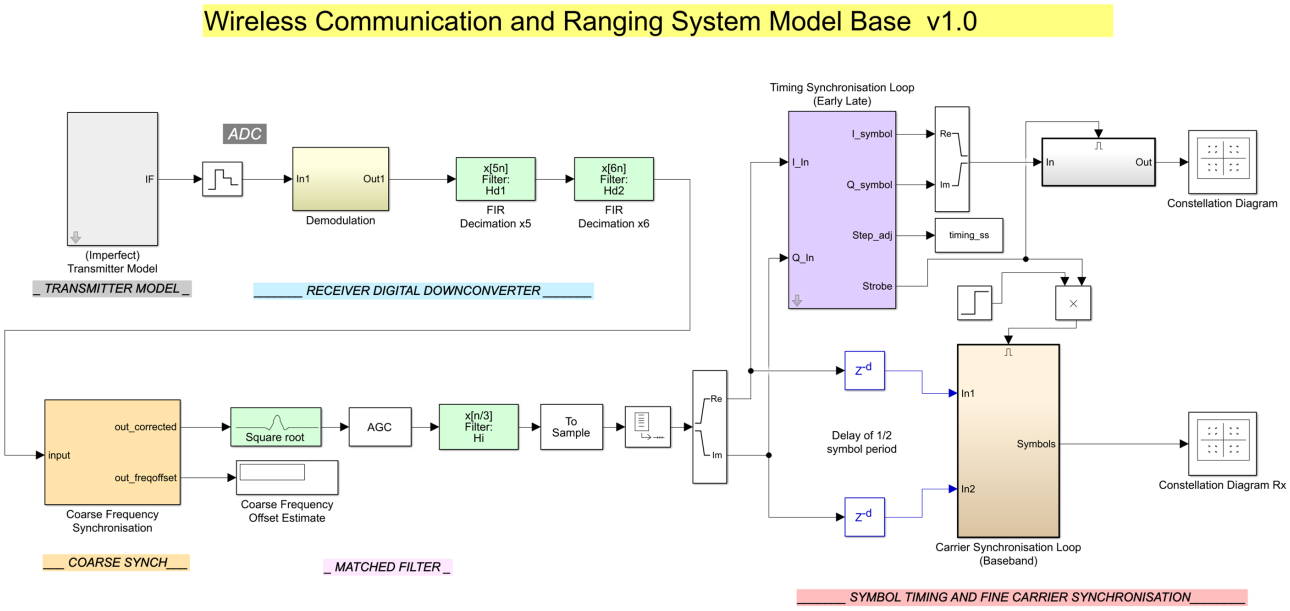

Figure 12. Simulation model of communication and measurement system.

5.2. Results and Analysis

(1) The data rate is fixed, and the QPSK BER simulation under different phase noise and different thermal noise conditions.

It can be seen from Figure 13 that under the condition of a fixed signal-to-noise ratio, the greater the phase noise, the greater the bit error rate. When the root mean square error of the phase noise sequence is 5°, to meet the bit error rate requirement of 1×10^{-5}, the required E_b/N_0 needs to be increased by 0.7 dB. When the root mean square error is 10°, E_b/N_0 needs to be improved by about 5 dB. When the phase noise is large to a certain extent, continuously improving the signal-to-noise ratio cannot reduce the bit error rate. As shown in the top curve in the figure, the root mean square of the phase noise is 20°. With the increase of E_b/N_0, the slope of the curve gradually decreases, that is, the phase noise deteriorates to a certain extent, and the communication system will not work properly.

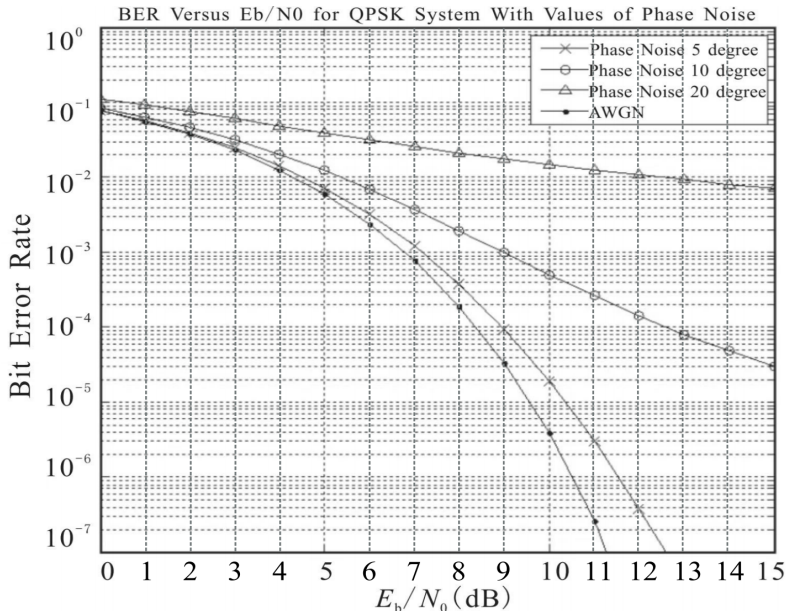

Figure 13. Signal-to-noise ratio vs. bit error rate under different phase noise level.

(2) The phase noise is fixed, and thermal noise affects the bit error rate of different transmission rates.

Taking the QPSK system as an example, the root mean square error of the phase noise in the time domain is 5°, as in Figure 14, and the influence of the phase noise on the transmission of the system under different data transmission rates is simulated. The simulation results are shown in Figure 15. Under this simulation condition, when the transmission rate is greater than 100 kbps, the system error deterioration is small. When the transmission rate is less than 100 bps, the system bit error is seriously deteriorated. Therefore, when the system phase noise index is poor, the low bit rate data transmission system is more susceptible to the influence of phase noise than the higher bit rate data transmission system.

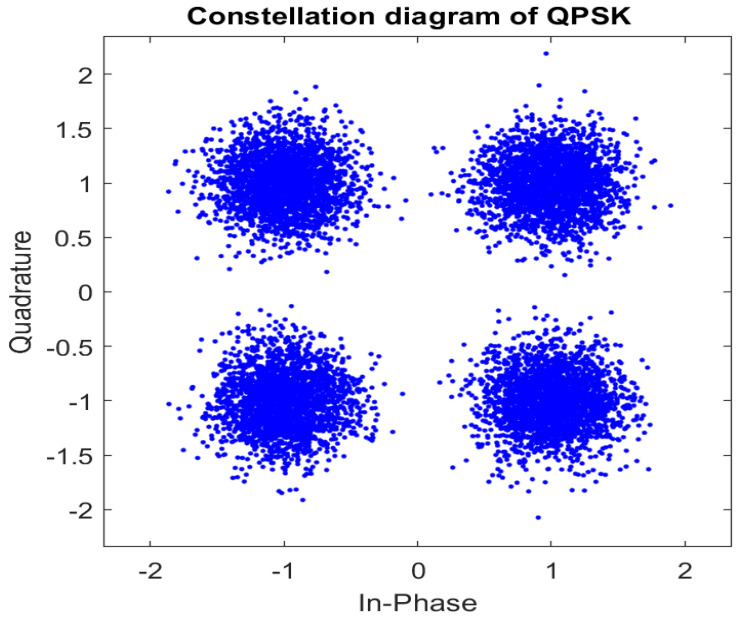

Figure 14. QPSK constellation diagram when phase noise RMS = 5°.

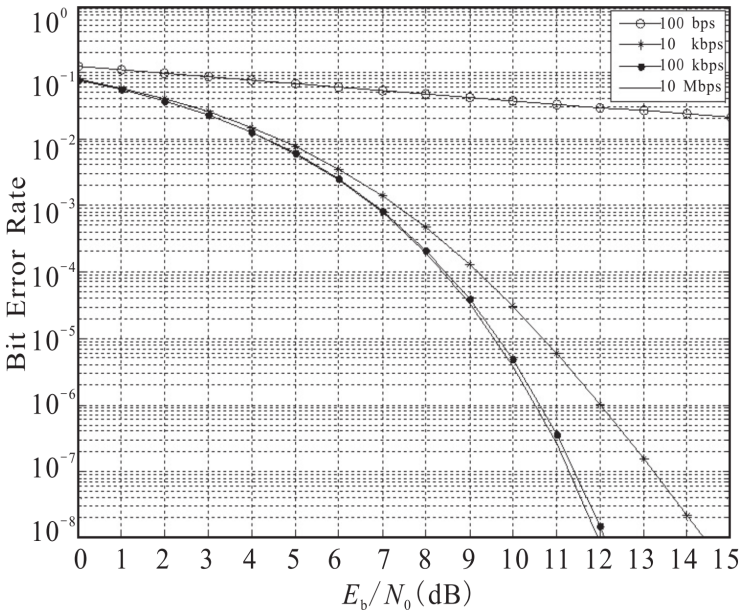

Figure 15. Bit error rate curves at different code rates using QPSK when phase noise RMS = 5°.

(3) Influence of phase noise on bit error rate under different modulation methods

Taking the phase root mean square error of 5° as an example, the simulation calculation is carried out for the BPSK, QPSK, 8PSK and 16QAM modulation modes, and compared with the respective theoretical values under the AWGN channel; it can be seen from the results in Figure 16 effect of phase noise. Accordingly, when designing a high-order modulation system, the phase noise index must be strictly required.

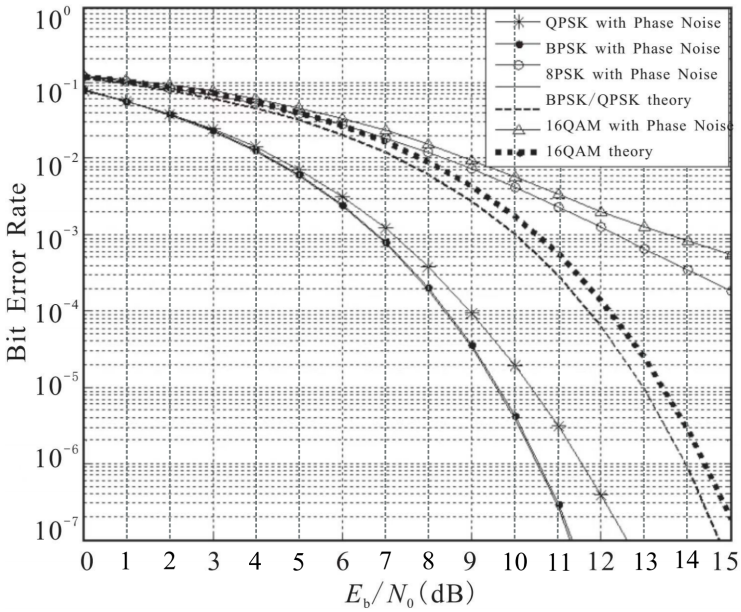

Figure 16. Bit error rate curve under different modulation methods when phase noise RMS = 5°.

6. Conclusions

In this paper, the theoretical model of phase noise and its simulation methods in frequency and time domains are firstly studied, and the power law spectrum model in the frequency domain and a typical method for solving phase noise jitter in the time domain are given. Then, for typical communication measurement systems, the two problems of phase-noise frequency-domain transfer and time-domain noise generation are studied, respectively. The frequency domain transfer function of phase noise in a carrier tracking loop is given, and the different effects of thermal noise and phase noise on the output of common third-order phase-locked loops are analyzed. A time-domain phase noise sequence generation algorithm based on discrete fractional integral operation is proposed. For the measured single-sideband phase noise spectrum of an OCXO, the proposed algorithm is used to generate the various order components of the power law spectral model and the integrated time-domain noise sequence, and the simulated SSB phase noise is generated by calculating again from this sequence. The result is in good agreement with the measured result of the instrument, which shows the effectiveness and accuracy of the algorithm. Finally, a communication measurement simulation system is built, and a discrete sequence simulation analysis method combining the frequency domain and time domain is provided, and the coupling relationship of key indicators such as phase noise, thermal noise, communication data rate, modulation method and bit error rate is synthesized. The results show that the bit error rate of the QPSK/BPSK communication system will not be significantly reduced if the phase jitter RMS caused by phase noise is less than 5 degrees, so 5 degrees can be used as a reference for the decomposition of the carrier SSB phase noise index. In addition, for modulation modes of 8PSK and higher order, the effect of phase noise is more significant, and the Eb/No index of the channel containing the phase noise is significantly increased compared with the case of the Gaussian white noise channel. The simulation gives some analysis results under the common technical indicators of the satellite inter-satellite link system, which provides an effective reference for the engineering design of a certain type of payload.

Author Contributions: Conceptualization, X.L., H.L. and X.W.; Methodology, X.L., Y.H., F.W. and X.W.; Software, H.L. and F.W.; Validation, X.L., Y.H. and F.W.; Formal analysis, H.L., Y.H., F.W. and C.Z.; Investigation, X.L., H.L., Y.H., F.W., C.Z. and X.W.; Resources, Y.H., C.Z. and X.W.; Data curation, X.L., H.L., Y.H., F.W. and C.Z.; Writing—original draft, X.L.; Writing—review & editing, C.Z. and X.W.; Visualization, C.Z. and X.W.; Supervision, H.L. and Y.H.; Project administration, X.W.; Funding acquisition, X.W. All authors have read and agreed to the published version of the manuscript.

Funding: This research was funding by China Aerospace Innovation Fund (21GFH-HT01-336).

Data Availability Statement: (1) The phase noise test data used to support the findings of this study are included within the article, listed below: (a) Typical Ka signal phase noise test results as Figure 3 and Table 1, which can be read out directly; (b) Power law spectrum parameters of a typical oscillator which is used to support the tracking error of PLL in Section 3 are included in Table 3; (c) Phase noise measurement of 5 MHz OCXO in Figure 8 is used to support Figures 9–11. All relevant data can be found in Section 4. (2) The simulation data used to support the findings of Section 5 are available from Matlab/Simulink.

Conflicts of Interest: The authors declare no conflict of interest.

References

1. Liu, J.X. The Effect of Phase Noise on BER of Data Transmission. *Telecommun. Eng.* **2007**, *45*, 63–65.
2. Song, W.; Ye, L. Research on the phase noise of the local oscillator and its influence on the performance of the receiver. *China New Telecommun.* **2019**, *21*, 40.
3. Zhu, L.B. Effect of Phase Noise on Demodulation Performance of QPSK System. *Radio Eng.* **2015**, *45*, 38–40.
4. Wang, Y.J.; Zhao, H.L.; Li, M.J. Analysis of Influence of Phase Noise on QPSK System Performance. *J. Nanjing Univ. Aeronaut. Astronaut.* **2010**, *42*, 68–71.
5. Guan, P.X.; Wang, Y.R.; Yu, H.K. Iterative Phase Noise Suppression for Full-Duplex Communication Systems. *China Commun.* **2023**, *20*, 226–234. [CrossRef]
6. Deng, X.J.; Yang, H.; Wu, Q.Y. Phase Noise Effects on the Performance of High-Order Digital Modulation Terahertz Communication System. *Chin. J. Electron.* **2022**, *31*, 589–594. [CrossRef]
7. Udayakumar, E.; Krishnaveni, V. Analysis of Phase Noise Issues in Millimeter Wave Systems for 5G Communications. *Anal. Phase Noise Issues Millim. Wave Syst. Commun.* **2022**, *126*, 1601–1619.
8. Quan, X.; Liu, Y.; Fan, P.Z. Full-Duplex Transceiver Design in the Presence of Phase Noise and Performance Analysis. *IEEE Trans. Veh. Technol.* **2021**, *70*, 558–571. [CrossRef]
9. Siddique, A.; Delwar, T.S.; Kurbanov, M.; Ryu, J.Y. Low-power low-phase noise VCO for 24 GHz applications. *Microelectron. J.* **2020**, *97*, 104720. [CrossRef]
10. Low complexity blind detection in OFDM systems with phase noise. *Digit. Signal Process.* **2022**, *129*, 103638. [CrossRef]
11. Zhu, K.; Wang, Y.; Wang, D. A low phase noise frequency synthesis method based on phase-locked loop array. In Proceedings of the 2023 International Conference on Microwave and Millimeter Wave Technology (ICMMT), Harbin, China, 12–15 August 2023; pp. 1–3. [CrossRef]
12. Wang, Q.; Ma, W.; Liu, L.; Qian, L.P.; Yang, X.; Kam, P.Y. Design and Performance Evaluation of Polar Coding for BICM Systems with Phase Noise. *IEEE Commun. Lett.* **2023**, *1*, 227–243. [CrossRef]
13. Xu, T.; Jin, C.; Zhang, S.; Jacobsen, G.; Popov, S.; Leeson, M.; Liu, T. Phase noise cancellation in coherent communication systems using a radio frequency pilot tone. *Appl. Sci.* **2019**, *9*, 4717. [CrossRef]
14. Wei, Z. Influence Analysis of Carrier Phase Noise on Modulation and Demodulation Performance in Satellite Communication Downlink. In *Signal and Information Processing, Networking and Computers*; Springer: Berlin/Heidelberg, Germany, 2021; pp. 238–246.
15. Quadri, A.; Zeng, H.; Hou, Y.T. A real-time mmwave communication testbed with phase noise cancellation. In Proceedings of the IEEE INFOCOM 2019-IEEE Conference on Computer Communications Workshops (INFOCOM WKSHPS), Paris, France, 29 April–2 May 2019; IEEE: Piscataway, NJ, USA, 2019; pp. 455–460.
16. Yu, Y.Z.; Lin, D.W.; Sang, T.H. Fast simulation of convolutionally coded communication system for performance evaluation with a novel noise gauging method. In Proceedings of the 2021 IEEE 93rd Vehicular Technology Conference (VTC2021-Spring), Helsinki, Finland, 25–28 April 2021; IEEE: Piscataway, NJ, USA, 2021; pp. 1–5.
17. Zhang, S.K.; Zhong, C.X.; Wang, H.B.; Yang, J. A New Method of Time Domain-Frequency Domain Parameter Conversion for Oscillator Stability. In Proceedings of the 2009 National Conference on Time and Frequency, Chengdu, China, 22 October 2009; pp. 403–411.
18. Ke, X.Z.; Wu, Z.S. Time-Frequency Domain Filtering of Oscillator Noise. *Electron. J.* **1998**, *26*, 126–128.
19. Feng, F.; Gong, H.; Zhang, W.C.; Chen, H.M. A method for designing the loop parameters of digital PLL based on equivalent signal model. *GNSS World China* **2021**, *46*, 93–100.
20. Kasdin, N.J. Discrete simulation of colored noise and stochastic processes and 1/f/sup/spl alpha//power law noise generation. *Proc. IEEE* **1995**, *83*, 802–827. [CrossRef]
21. Murgulescu, M.H. A Lesson-like convergent equation for the phase noise of an oscillator with 1/f noise. *Microw. Opt. Technol. Lett.* **2020**, *62*, 1200–1203. [CrossRef]
22. Donnelly, Y.; Kennedy, M.P. Prediction of phase noise and spurs in a nonlinear Fractional-{*N*} frequency synthesizer. *IEEE Trans. Circuits Syst. I Regul. Pap.* **2019**, *66*, 4108–4121. [CrossRef]

23. Ugolini, A.; Piemontese, A.; Eriksson, T. Spiral constellations for phase noise channels. *IEEE Trans. Commun.* **2019**, *67*, 7799–7810. [CrossRef]
24. Taggart, D.; Kumar, R. Impact of phase noise on the performance of the QPSK modulated signal. In Proceedings of the 2011 Aerospace Conference, Big Sky, MT, USA, 5–12 March 2011; IEEE: Piscataway, NJ, USA, 2011; pp. 1–10.

Disclaimer/Publisher's Note: The statements, opinions and data contained in all publications are solely those of the individual author(s) and contributor(s) and not of MDPI and/or the editor(s). MDPI and/or the editor(s) disclaim responsibility for any injury to people or property resulting from any ideas, methods, instructions or products referred to in the content.